A Comprehensive Analysis of Mapping Functions Used in Modeling Tropospheric Propagation Delay in Space Geodetic Data[1]

V.B. Mendes and R.B. Langley
Geodetic Research Laboratory
Department of Geodesy and Geomatics Engineering
University of New Brunswick
Fredericton, N.B. E3B 5A3
e-mail: lang@unb.ca

[1]Paper presented at KIS94, International Symposium on Kinematic Systems in Geodesy, Geomatics and Navigation, Banff, Canada, August 30 – September 2, 1994.

BIOGRAPHIES

Virgílio Mendes received his Diploma in Geographic Engineering from the Faculty of Sciences of the University of Lisbon, Portugal, in 1987. Since then, he has been working as a teaching assistant at this university. In 1990, he completed the Specialization Course in Hydrography at the Hydrographic Institute, Lisbon. In 1991, he enrolled as a Ph. D. student at the University of New Brunswick. He is involved in the application of the Global Positioning System to the monitoring of crustal deformation.

Richard Langley is a professor in the Department of Geodesy and Geomatics Engineering at the University of New Brunswick, where he has been teaching since 1981. He has a B.Sc. in applied physics from the University of Waterloo and a Ph.D. in experimental space science from York University, Toronto. After obtaining his Ph.D., Dr. Langley spent two years with the Department of Earth and Planetary Sciences of the Massachusetts Institute of Technology where he carried out research involving lunar laser ranging and very long baseline interferometry.

Dr. Langley has worked extensively with the Global Positioning System. He is a co-author of the best-selling Guide to GPS Positioning published by Canadian GPS Associates and is a columnist for GPS World magazine. He has helped develop and present a number of seminar courses on GPS for both Canadian GPS Associates and the American-based Navtech Seminars Inc. Dr. Langley has consulted extensively in the field of GPS with private companies and government agencies both in Canada and abroad.

ABSTRACT

The principal limiting error source in the Global Positioning System and other modern space geodesy techniques, such as very long baseline interferometry, is the mismodeling of the delay experienced by radio waves in propagating through the electrically neutral atmosphere, usually referred to as the tropospheric delay. This propagation delay is generally split into two components, called hydrostatic (or dry) and wet, each of which can be described as a product of the delay at the zenith and a mapping function, which models the elevation dependence of the propagation delay.

In the last couple of decades, a number of mapping functions have been developed for use in the analysis of space geodetic data. Using ray tracing through an extensive radiosonde data set covering different climatic regions as "ground truth", an assessment of accuracy of most of these mapping functions, including those developed by Saastamoinen, Lanyi, Davis (CfA-2.2), Santerre, Ifadis, Baby, Herring (MTT), and Niell (NMF), has been performed. The ray tracing was performed for different elevation angles, starting at 3°.

Virtually all of the tested mapping functions provide sub-centimeter accuracy for elevation angles above 15°. However, stochastic techniques currently used to model the tropospheric zenith delay require low elevation observations in order to reduce the correlation between the estimates of the zenith tropospheric delay and the station height. Based on this analysis, and for elevation angles below 10°, only a select few of the mapping functions were found to adequately meet the requirements imposed by the space geodetic techniques.

INTRODUCTION

The electromagnetic signals used by modern space geodetic techniques propagate through part of the earth's atmosphere – specifically through an ionized layer (the ionosphere) and a layer that is electrically neutral, composed primarily of the troposphere and stratosphere, referred to as the neutral atmosphere. Unlike the ionized part of the atmosphere, the neutral atmosphere is essentially a non-dispersive medium at radio frequencies (except for the anomalous dispersion of the water vapor and oxygen spectral lines), i.e., the effects on phase and group delay are equivalent and the availability of more than one transmitted frequency is of no advantage in removing the tropospheric effect. Since the troposphere accounts for most of the neutral atmosphere mass and contains practically all the water vapor, the term *tropospheric delay* is often used to designate the global effect of the neutral atmosphere. The effect of the neutral atmosphere is a major residual error source in modern space geodesy techniques, such as the Global Positioning System (GPS), very long baseline interferometry (VLBI), Doppler Orbitography and Radiopositioning Integrated by Satellite (DORIS), satellite altimetry (as featured on the TOPEX/Poseidon and SEASAT satellites), and satellite laser ranging (SLR).

The neutral atmosphere affects the propagation of microwaves, causing a propagation delay and, to a lesser extent, bending of the ray path. These effects depend on the real-valued *refractive index*, n, along the signal ray path, more conveniently expressed by another quantity, the *refractivity*, N:

$$N = (n-1)\cdot 10^6, \tag{1}$$

which can be expressed, in general, as [Thayer, 1974]

$$N = K_1\left(\frac{P_d}{T}\right)Z_d^{-1} + \left[K_2\left(\frac{e}{T}\right) + K_3\left(\frac{e}{T^2}\right)\right]Z_w^{-1}, \tag{2}$$

where P_d is the partial pressure of the dry gases in the atmosphere, e is the partial pressure of the water vapor, T is the absolute temperature, Z_d is the compressibility factor for dry air, Z_w is the compressibility factor for water vapor, and K_i are constants empirically determined.

The compressibility factors are corrections to account for the departure of the air behavior from that of an ideal gas and depend on the partial pressure due to dry gases and temperature [Owens, 1967]. The most often used sets of refractivity constants are the ones provided by Smith and Weintraub [1953] and Thayer [1974] (see Table 1).

	Smith and Weintraub [1953]	Thayer [1974]
K_1	77.61±0.01	77.60±0.014
K_2	72±9	64.8±0.08
K_3	$(3.75\pm0.03)\cdot10^5$	$(3.776\pm0.004)\cdot10^5$

Table 1 - Experimentally determined values for the refractivity constants (K_1 and K_2 are in $K\cdot mbar^{-1}$, K_3 is in $K^2\cdot mbar^{-1}$).

The tropospheric delay contribution d_{trop} to a radio signal propagating from a satellite to the earth's surface is given in first approximation by [Langley, 1992]:

$$d_{trop} = \int_{r_s}^{r_a}[n(r)-1]\csc\theta(r)\ dr + d_{geo}, \tag{3}$$

where d_{geo} is the geometric delay that accounts for the difference between the refracted and rectilinear ray paths (ray bending), given by

$$d_{geo} = \left[\int_{r_s}^{r_a}\csc\theta(r)\ dr - \int_{r_s}^{r_a}\csc\ \varepsilon(r)\ dr\right],$$

and where r is the geocentric radius, θ is the refracted (apparent) satellite elevation angle, ε is the non-refracted (geometric or true) satellite elevation angle, r_s is the geocentric radius of the earth's surface, and r_a is the geocentric radius of the top of the neutral atmosphere.

This equation is valid for a spherically symmetric atmosphere, for which n varies simply as a function of the geocentric radius. The first integral in equation (3) represents the difference between the electromagnetic and geometric lengths of the refracted transmission path. For a signal coming from the zenith direction, the geometric delay is zero; hence, for a spherically symmetric atmosphere equation (3) becomes at the zenith:

$$d_{trop}^z = \int_{r_s}^{r_a}[n(r)-1]\ dr = 10^{-6}\int_{r_s}^{r_a}N\ dr. \tag{4}$$

The delay just defined is the tropospheric *zenith delay*. The integration of the total refractivity expressed by equation (2) depends on the mixing ratio of moist air. As shown in Davis et al. [1985], it is possible to derive a new refractivity definition for which the first term is dependent on the total mass density ρ only. Following this formalism, the total refractivity can be expressed as the sum of a hydrostatic component (versus dry component using the formalism expressed in equation (2)) and a wet component:

$$N = K_1 R_d \rho + \left[K_2^{'} \left(\frac{e}{T} \right) + K_3 \left(\frac{e}{T^2} \right) \right] Z_w^{-1}, \qquad (5)$$

where R_d is the specific gas constant for dry air, and $K_2^{'}$ = (17±10) K·mbar^{-1} [Davis et al., 1985].

The zenith delay can be related to the delay that the signal would experience at other elevation angles through the use of *mapping functions*. If the mapping functions are determined separately for the hydrostatic and the wet component, the tropospheric delay can be expressed as:

$$d_{trop} = d_h^z \cdot m_h(\varepsilon) + d_w^z \cdot m_w(\varepsilon) \qquad (6)$$

where d_h^z is the zenith delay due to dry gases, d_w^z is the zenith delay due to water vapor, m_h is the hydrostatic component mapping function, m_w is the wet component mapping function and ε, as above, is the non-refracted elevation angle at the ground station (some mapping functions use the refracted angle, θ).

A recent advance in estimation techniques (especially in VLBI) is the inclusion of observations at low elevation angles, which reduce the correlation between the estimates of the zenith atmospheric delay and the station heights [e.g. Rogers et al., 1993]. Lichten [1990] also found that GPS baseline repeatability improves when low elevation GPS data is included in the estimation process. There is some irony here: errors in the mapping functions, which increase at low elevation angles, can induce systematic errors in the estimation of the tropospheric delay, which will introduce errors in the vertical component of the estimated positions; on the other hand, the inclusion of low elevation observations will likely improve the precision of the baseline vector estimates [e.g. Davis et al., 1991; MacMillan and Ma, 1994]. This constant need for better mapping functions in the analysis of space geodetic data was the motivation for the assessment of fifteen mapping functions through comparison with ray tracing through radiosonde data. The mapping functions assessed in this study and the corresponding codes used in the tables of results are listed in Table 2.

The mapping functions were tested for the standard formulations specified by the authors. Site-optimized mapping functions, such as those derived by Ifadis [1986], and additional functions by Chao [Estefan, 1994], for example, are not included in our analysis. The latter represent a significant improvement over the original function tested here, but remain unpublished.

The original model developed by Hopfield [1969] and a model developed by Rahnemoon [1988] are not included in this analysis. The first is numerically stable only if computed in quadruple precision; using ray tracing through standard profiles, we found [Mendes and Langley, 1994] that its accuracy is very similar to that provided by the Yionoulis algorithm, as expected. The second is a numerical-integration-based model, for which an explicit product of a zenith delay and a mapping function can be formed only artificially.

CODE	REFERENCE
BB	Baby et al. [1988]
BL	Black [1978]
BE	Black and Eisner [1984]
CH	Chao [1972]
DA	Davis et al. [1985]
GG	Goad and Goodman [1974]
HE	Herring [1992]
HM	Moffett [1973]
IF	Ifadis [1986]
LA	Lanyi [1984]
MM	Marini and Murray [1973]
NI	Niell [1993a,1993b,1994]
SA	Saastamoinen [1973]
ST	Santerre [1987]
YI	Yionoulis [1970]

Table 2 - List of the mapping functions. (Note: BL, BE, GG, HM, ST, and YI are based on the Hopfield [1969] model; CH, DA, HE, IF, MM, and NI are based on the Marini [1972] continued fraction form.)

Typographical errors in some publications (e.g. Ifadis [1986], Lanyi [1984], Baby et al. [1988]) were corrected [Ifadis, 1994; Cazenave, 1994]. Whenever required, we used nominal values for the temperature lapse rate (6.5 K/km) and tropopause height (11 231 m – a value suggested in Davis et al. [1985]). For the case of the Baby et al. (hereafter simply called Baby) and Saastamoinen functions, the apparent elevation angle rather than the geometric elevation angle was used, as required by the functions.

RAY TRACING

To compute the tropospheric delay components to be used as benchmark values, radiosonde data from nine stations (see Table 3) representing different climatic regions was used. The data pertains to the year 1992, each station having typically two balloon launches per day, at 11 h and 23 h UT (U.S. controlled stations) and 0 h and 12 h UT (Canadian stations), and consist of height profiles of pressure, temperature and relative humidity. Radiosonde profiles with obvious errors (e.g. no surface data recorded) were discarded.

For each ray trace, the hydrostatic and the wet components of the tropospheric delay were computed separately using the refractivity constants determined by Thayer [1974] and the hydrostatic/wet formalism expressed in Davis et al. [1985]. The geometric delay (ray bending term) was added to the hydrostatic component. The mean and the root-mean-square (rms) about the mean of the NP values of the hydrostatic and wet components of the zenith delay computed from the ray traces for each station are shown in Table 4.

STATION	φ (°N)	λ (°W)	H (m)	NP
San Juan	18.43	66.10	3	675
Guam	13.55	215.17	111	736
Nashville	36.12	86.68	180	745
Denver	39.75	108.53	1611	753
Oakland	37.73	122.20	6	740
St. John's	47.62	52.75	140	713
Whitehorse	60.72	135.07	704	719
Kotzebue	66.87	162.63	5	687
Alert	82.50	62.33	66	720

Table 3 - Approximate locations of the radiosonde sites and the corresponding number of profiles (NP) used. H is the height of the station above the geoid.

RESULTS AND CONCLUSIONS

The results of our assessment are summarized in Tables 5 to 9. In Tables 5 to 8, the mean values of the differences between the delays computed using the mapping functions and the ray-trace results corresponding to elevation angles of 30°, 15°, 10° and 3° (and separately for the hydrostatic, wet, and total delay) are listed; the rms differences for the total delay only, and for the same elevation angles, are listed in Table 9.

Although some of the mapping functions were designed to model observations above a certain elevation angle, results for lower elevation angles are presented for illustrative purposes. It should be pointed out that the values tabulated represent the differences due to mapping-function errors only, a different approach than that used by Janes et al. [1991].

	HYD (m)		WET (m)	
STATION	mean	rms	mean	rms
San Juan	2.316	0.005	0.264	0.045
Guam	2.281	0.009	0.274	0.062
Nashville	2.270	0.012	0.151	0.081
Denver	1.908	0.012	0.073	0.040
Oakland	2.313	0.010	0.115	0.035
St. John's	2.268	0.026	0.092	0.056
Whitehorse	2.108	0.021	0.060	0.031
Kotzebue	2.299	0.025	0.056	0.042
Alert	2.282	0.022	0.032	0.023

Table 4 - Statistical summary of the ray traces for the hydrostatic (HYD) and wet components of the zenith delay for the different radiosonde stations.

For the total delay, virtually all of the tested mapping functions have discrepancies with respect to the ray-tracing results of less than 5 mm for elevation angles above 30°, but only the Baby, Herring, Ifadis, Lanyi, and Niell mapping functions showed submillimeter accuracy. The lack of correction values for elevation angles at 30° and above in the Saastamoinen mapping function explains a comparatively better performance of the function at 15° for most of the sites.

For elevation angles above 10°, the performance of the mapping functions can be classified into three major groups. The least satisfactory performance is shared by the Hopfield-based functions and the Marini-Murray mapping function. For this first group, the great part of the discrepancies is due to the disregard of the geometric delay inherent in the definition of the tropospheric delay. The mapping function developed by Santerre [1987] represents a substantial improvement over the rest of the group. The best performances are achieved by the remaining functions based on the Marini [1972] continued fraction form, and by the Baby, Lanyi, and Saastamoinen functions. Both the Lanyi and Davis mapping function differences with respect to ray tracing indicate some seasonal and/or latitude dependence, which might be caused by the use of nominal values for the tropopause height and temperature lapse rate. As those parameters are generally not known exactly, the procedure of using nominal values is likely the one that will be used in the implementations of these mapping functions in software for most space geodetic data analyses.

Among the group of models performing the best, the precision of the Niell, Herring, and Ifadis mapping functions stands out even at high elevation angles and it is quite remarkable at very low elevation angles (less than about 10°), showing biases with respect to the "benchmark" ray-trace values which are about one to two orders of magnitude smaller than those obtained using other functions. The Niell and Ifadis functions have smaller biases than Herring's at low elevation angles, but Ifadis' functions show less scatter than Niell's. The worst performance of the Niell mapping functions, both in terms of bias and long-term scatter, happens for high latitudes. The phenomena of temperature inversions affect some of the models and is responsible for the large short-term scatter shown by those mapping functions using temperature as a parameter. In these cases, the surface temperature value driving the models is not representative of the conditions aloft, resulting in a biased determination of the delay (see Figure 1). Although some of the functions were designed to be used for elevation angles above 10°, only the Baby and Saastamoinen functions break down very rapidly below this limit, as illustrated in Table 8.

Based on our analysis, we conclude that a large number of mapping functions can provide satisfactory results when used for elevation angles above 15°. For high-precision applications, it is recommended that the mapping functions derived by Lanyi, Herring, Ifadis or Niell be used. The last three functions are more accurate than the first at lower elevation angles and are more effective in terms of ease of implementation and computation speed. Neverthless, and according to our analysis, errors can still be induced by these four mapping functions at low elevation angles (of the order of tens of centimeters at 3°).

ACKNOWLEDGMENTS

We would like to express our appreciation to Arthur Niell for providing the source code for the NMF (Niell) mapping functions and the ray-trace software (developed by James Davis, Thomas Herring, and Arthur Niell) and to Thomas Herring for the source code of the MTT (Herring) mapping functions. We also thank Anne Cazenave for helping to clarify the formulation in the Baby mapping function.

The support of the *Programa Ciência/Junta Nacional de Investigação Científica e Tecnológica*, Portugal, and the University of New Brunswick's University Research Fund is gratefully acknowledged.

REFERENCES

Baby, H.B., P. Golé, and J. Lavergnat (1988). "A model for the tropospheric excess path length of radio waves from surface meteorological measurements." *Radio Science*, Vol. 23, No. 6, pp. 1023-1038.

Black, H.D. (1978). "An easily implemented algorithm for the tropospheric range correction." *Journal of Geophysical Research*, Vol. 38, No. B4, pp. 1825-1828.

Black, H.D and A. Eisner (1984). "Correcting satellite Doppler data for tropospheric effects." *Journal of Geophysical Research*, Vol. 89, No. D2, pp. 2616-2626.

Cazenave, A. (1994). Personal communication. Groupe de Recherche de Géodésie Spatiale, Toulouse, France.

Chao, C.C. (1972). "A model for tropospheric calibration from daily surface and radiosonde balloon measurements." JPL Technical Memorandum 391-350, Jet Propulsion Laboratory, Pasadena, CA.

Davis, J.L., T.A. Herring, I.I. Shapiro, A.E.E. Rogers, and G. Elgered (1985). "Geodesy by radio interferometry: effects of atmospheric modeling errors on estimates of baseline length." *Radio Science*, Vol. 20, No. 6, pp. 1593-1607.

Davis, J.L., T.A. Herring, and I.I. Shapiro (1991). "Effects of atmospheric modeling errors on determinations of baseline vectors from very long baseline interferometry." *Journal of Geophysical Research*, Vol. 96, No. B1, pp. 643-650.

Estefan, J. (1994). Personal communication. Jet Propulsion Laboratory, Pasadena, CA.

Goad, C.C. and L. Goodman (1974). "A modified Hopfield tropospheric refraction correction model." Paper presented at the AGU Annual Fall Meeting, San Francisco, CA, Dec. 12-17 (abstract: EOS, Vol. 55, p. 1106, 1974).

Herring, T.A. (1992). "Modeling atmospheric delays in the analysis of space geodetic data." *Proceedings of the Symposium on Refraction of Transatmospheric Signals in Geodesy*, Eds. J.C. De Munck and T.A.Th. Spoelstra, Netherlands Geodetic Commission, Publications on Geodesy, No. 36, pp. 157-164.

Hopfield, H.S. (1969). "Two-quartic tropospheric refractivity profile for correcting satellite data." *Journal of Geophysical Research*, Vol. 74, No. 18, pp. 4487-4499.

Ifadis, I.I. (1986). "The atmospheric delay of radio waves: modeling the elevation dependence on a global scale." Technical Report 38L, Chalmers University of Technology, Göteborg, Sweden.

Ifadis, I.I. (1994). Personal communication. Aristotle University of Thessaloniki, Department of Civil Engineering, Division of Geotechnical Engineering, Section of Geodesy, Thessaloniki, Greece.

Janes, H.W., R.B. Langley, and S.P. Newby (1991). "Analysis of tropospheric delay prediction models:

comparisons with ray-tracing and implications for GPS relative positioning." *Bulletin Géodésique*, Vol. 65, pp. 151-161.

Lanyi, G. (1984). "Tropospheric delay effects in radio interferometry." *Telecommunications and Data Acquisition Progress,* JPL Technical Report 42-78, Jet Propulsion Laboratory, Pasadena, CA, pp. 152-159.

Langley, R.B. (1992). "The effect of the ionosphere and troposphere on satellite positioning systems." Paper presented at the Symposium on Refraction of Transatmospheric Signals in Geodesy, The Hauge, The Netherlands, May 19-22.

Lichten, S.M. (1990). "Precise estimation of tropospheric path delays with GPS techniques." *Telecommunications and Data Acquisition Progress Report*, JPL Technical Report 42-100, Jet Propulsion Laboratory, Pasadena, California.

Marini, J.W. (1972). "Correction of satellite tracking data for an arbitrary tropospheric profile." *Radio Science*, Vol. 7, No. 2, pp. 223-231.

Marini, J.W. and C.W. Murray (1973). "Correction of laser range tracking data for atmospheric refraction at elevations above 10 degrees." Goddard Space Flight Center Report X-591-73-351, NASA GSFC, Greenbelt, MD.

MacMillan, D.S. and C. Ma (1994). "Evaluation of very long baseline interferometry atmospheric modeling improvements." *Journal of Geophysical Research*, Vol. 99, No. B1, pp. 637-651.

Mendes, V.B. and R.B. Langley (1994). "Modeling the tropospheric delay from meteorological surface measurements: comparison of models." Presented at the American Geophysical Union Spring Meeting, MD, 23-27 May 1994 (abstract: EOS, Vol. 75, No. 16, Spring Meeting Supplement, p. 105, 1994).

Moffett, J.B. (1973). "Program requirements for two-minute integrated Doppler satellite navigation solution." Technical Memorandum TG 819-1, Applied Physics Laboratory, The Johns Hopkins University, Laurel, MD.

Niell, A.E. (1993a). "A new approach for the hydrostatic mapping function." *Proceedings of the International Workshop for Reference Frame Establishment and Technical Development in Space Geodesy*, Communications Research Laboratory, Koganei, Tokyo, Japan, 18-21 January 1993, pp. 61-68.

Niell, A. E. (1993b). "Improved global atmospheric mapping functions for VLBI and GPS." *URSI/IAU Symposium on VLBI Technology - Progress and Future Observational Possibilities*, Kyoto, Japan, 6-10 September 1993 (abstract).

Niell, A.E. (1994). Personal communication. Haystack Observatory, Westford, MA.

Owens, J.S. (1967). "Optical refractive index of air: dependence on pressure, temperature, and composition." *Applied Optics*, Vol. 6, No. 1, pp. 51-59.

Rahnemoon, M. (1988). *Ein neues Korrekturmodell für Mikrowellen - Entfernungsmessungen zu Satelliten*. Deutsche Geodätische Kommission, Reihe C, Heft Nr. 335, München, Germany.

Rogers, A.E.E., R.J. Cappallo, B.E. Corey, H.F. Hinteregger, A.E. Niell, R.B. Phillips, D.L. Smythe, A.R. Whitney, T.A. Herring, J.M. Bosworth, T.A. Clark, C. Ma, J.W. Ryan, J.L. Davis, I.I. Shapiro, G. Elgered, K. Jaldehag, J.M. Johansson, B.O. Rönnäng, W.E. Carter, J.R. Ray, D.S. Robertson, T.M. Eubanks, K.A. Kingham, R.C. Walker, W.E. Himwich, C.E. Kuehn, D.S. MacMillan, R.I. Potash, D.B. Shaffer, N.R. Vandenberg, J.C. Webber, R.L. Allshouse, B.R. Schupler, and D. Gordon (1993). "Improvements in the accuracy of geodetic VLBI." In *Contributions of Space Geodesy to Geodynamics: Technology*, Eds. D.E. Smith and D.L. Turcotte, Geodynamics Series, Vol. 25, American Geophysical Union, Washington, D.C. , pp. 47-62.

Saastamoinen, J. (1973). "Contributions to the theory of atmospheric refraction." In three parts. *Bulletin Géodésique*, No. 105, pp. 279-298; No. 106, pp. 383-397; No. 107, pp. 13-34.

Santerre, R. (1987). "Modification to the Goad & Goodman tropospheric refraction model." Unpublished internal report of the Department of Surveying Engineering, University of New Brunswick, Fredericton, N.B., Canada.

Smith, E.K. and S. Weintraub (1953). "The constants in the equation of atmospheric refractive index at radio frequencies." *Proceedings of the Institute of Radio Engineers*, Vol. 41, No. 8, pp. 1035-1037.

Thayer, G.D. (1974). "An improved equation for the radio refractive index of air." *Radio Science*, Vol. 9, No. 10, pp. 803-807.

Yionoulis, S.M. (1970). "Algorithm to compute tropospheric refraction effects on range measurements." *Journal of Geophysical Research*, Vol. 75, No. 36, pp. 7636-7637.

STATION		BB	BL	BE	CH	DA	GG	HE	HM	IF	LA	MM	NI	SA	ST	YI
		MAPPING FUNCTION														
SAN JUAN	H	-	1.6	-	-3.8	-1.7	1.6	0.0	2.9	-0.2	-	-	0.0	-	1.0	1.8
	W	-	0.4	-	0.3	-1.2	0.4	0.0	0.3	0.0	-	-	0.0	-	0.4	1.6
	T	**0.8**	**2.0**	**2.9**	**-3.5**	**-2.9**	**2.0**	**0.0**	**3.2**	**-0.2**	**-0.2**	**3.1**	**0.0**	**-3.2**	**1.4**	**3.4**
GUAM	H	-	1.6	-	-3.7	-1.7	1.6	0.0	2.9	-0.2	-	-	0.0	-	0.9	1.7
	W	-	0.4	-	0.3	-1.3	0.5	0.0	0.4	0.0	-	-	0.0	-	0.4	1.0
	T	**1.0**	**2.0**	**2.9**	**-3.4**	**-3.0**	**2.1**	**0.0**	**3.3**	**-0.2**	**-0.2**	**3.2**	**0.0**	**-3.1**	**1.4**	**2.7**
NASHVILLE	H	-	1.8	-	-4.1	-1.4	1.8	0.0	2.5	-0.2	-	-	-0.1	-	1.2	1.9
	W	-	0.2	-	0.2	-0.7	0.2	0.0	0.2	0.0	-	-	0.0	-	0.2	2.5
	T	**-0.3**	**2.0**	**2.8**	**-3.9**	**-2.1**	**2.0**	**0.0**	**2.7**	**-0.2**	**0.1**	**2.5**	**-0.1**	**-2.9**	**1.4**	**4.4**
DENVER	H	-	1.3	-	-3.9	-1.3	1.3	0.0	1.7	-0.2	-	-	0.0	-	0.8	1.4
	W	-	0.1	-	0.1	-0.3	0.1	0.0	0.1	0.0	-	-	0.0	-	0.1	1.3
	T	**-0.8**	**1.4**	**2.0**	**-3.8**	**-1.6**	**1.4**	**0.0**	**1.8**	**-0.2**	**-0.1**	**-1.8**	**0.0**	**-1.8**	**0.9**	**2.7**
OAKLAND	H	-	1.9	-	-4.1	-1.4	1.9	0.0	2.6	-0.2	-	-	0.0	-	1.2	2.0
	W	-	0.2	-	0.1	-0.5	0.2	0.0	0.1	0.0	-	-	0.0	-	0.2	2.2
	T	**0.0**	**2.1**	**3.0**	**-4.0**	**-1.9**	**2.1**	**0.0**	**2.7**	**-0.2**	**0.1**	**2.3**	**0.0**	**-3.0**	**1.4**	**4.2**
ST. JOHN'S	H	-	2.1	-	-4.3	-1.1	2.1	0.1	2.2	-0.1	-	-	-0.1	-	1.5	2.2
	W	-	0.1	-	0.1	-0.4	0.1	0.0	0.1	0.0	-	-	0.0	-	0.1	1.7
	T	**-0.5**	**2.2**	**2.7**	**-4.2**	**-1.5**	**2.2**	**0.1**	**2.3**	**-0.1**	**0.4**	**1.9**	**-0.1**	**-3.2**	**1.6**	**3.9**
WHITEHORSE	H	-	1.8	-	-4.4	-1.1	1.8	0.0	1.7	-0.2	-	-	0.0	-	1.2	1.9
	W	-	0.1	-	0.1	-0.3	0.1	0.0	0.1	0.0	-	-	0.0	-	0.1	1.1
	T	**-0.8**	**1.9**	**2.2**	**-4.3**	**-1.4**	**1.9**	**0.0**	**1.8**	**-0.2**	**0.2**	**1.5**	**0.0**	**-2.9**	**1.3**	**3.0**
KOTZEBUE	H	-	2.4	-	-4.7	-0.8	2.4	0.1	2.0	-0.2	-	-	-0.1	-	1.7	2.5
	W	-	0.1	-	0.1	-0.2	0.1	0.0	0.1	0.0	-	-	0.0	-	0.1	1.1
	T	**-0.5**	**2.5**	**2.5**	**-4.6**	**-1.0**	**2.5**	**0.1**	**2.1**	**-0.2**	**0.6**	**1.4**	**-0.1**	**-3.6**	**1.8**	**3.6**
ALERT	H	-	2.7	-	-5.0	-0.5	2.7	0.2	1.6	-0.2	-	-	-0.3	-	2.0	2.8
	W	-	0.1	-	0.0	-0.1	0.0	0.0	0.0	0.0	-	-	0.0	-	0.0	0.6
	T	**-0.5**	**2.8**	**2.2**	**-5.0**	**-0.6**	**2.7**	**0.2**	**1.6**	**-0.2**	**0.9**	**1.1**	**-0.3**	**-3.9**	**2.0**	**3.4**

Table 5 - Mapping function mean error at 30 degrees elevation angle. The values represent the mean differences between the delay computed using the different mapping functions and the ray-trace results, for the hydrostatic (H), wet (W) and total (T) delay, in millimetres. The BB, BE, LA, MM, and SA functions do not have separate hydrostatic and wet components.

STATION		MAPPING FUNCTION														
		BB	BL	BE	CH	DA	GG	HE	HM	IF	LA	MM	NI	SA	ST	YI
SAN JUAN	H	-	13.6	-	-5.2	0.9	13.3	-0.1	31.3	-1.6	-	-	-0.1	-	7.8	13.6
	W	-	3.5	-	3.4	-8.8	3.8	0.0	3.2	0.2	-	-	0.2	-	3.5	4.2
	T	**7.0**	**17.1**	**22.6**	**-1.8**	**-7.9**	**17.1**	**-0.1**	**34.5**	**-1.4**	**-2.3**	**26.4**	**0.1**	**-1.7**	**11.4**	**17.8**
GUAM	H	-	12.9	-	-4.9	0.7	12.6	0.0	31.1	-1.5	-	-	0.2	-	7.4	13.0
	W	-	3.7	-	3.6	-9.1	4.0	0.2	3.5	0.4	-	-	0.3	-	3.7	4.4
	T	**8.2**	**16.6**	**22.4**	**-1.3**	**-8.4**	**16.6**	**0.2**	**34.6**	**-1.1**	**-2.4**	**26.8**	**0.5**	**-1.5**	**11.1**	**17.4**
NASHVILLE	H	-	14.9	-	-7.8	2.4	14.8	0.2	28.0	-1.1	-	-	-0.6	-	9.4	15.0
	W	-	2.0	-	1.9	-4.9	1.9	0.1	1.8	0.2	-	-	0.1	-	1.8	2.4
	T	**-1.8**	**16.9**	**21.8**	**-5.9**	**-2.5**	**16.7**	**0.3**	**29.8**	**-0.9**	**0.0**	**20.7**	**-0.5**	**0.4**	**11.2**	**17.4**
DENVER	H	-	10.4	-	-10.3	0.9	10.4	0.2	19.8	-1.3	-	-	-0.2	-	6.4	10.5
	W	-	0.7	-	0.7	-2.5	0.7	0.1	0.7	0.0	-	-	-0.2	-	0.7	0.9
	T	**-6.4**	**11.1**	**15.5**	**-9.6**	**-1.6**	**11.1**	**0.3**	**20.5**	**-1.3**	**-0.9**	**15.1**	**-0.4**	**2.9**	**7.1**	**11.4**
OAKLAND	H	-	15.4	-	-7.4	2.5	15.4	0.2	29.1	-0.9	-	-	-0.1	-	9.7	15.5
	W	-	1.4	-	1.4	-3.8	1.8	0.0	1.3	0.0	-	-	0.0	-	1.7	1.7
	T	**0.6**	**16.8**	**23.6**	**-6.0**	**-1.3**	**17.2**	**0.2**	**30.4**	**-0.9**	**0.1**	**19.7**	**-0.1**	**0.1**	**11.4**	**17.2**
ST. JOHN'S	H	-	17.5	-	-10.2	4.8	17.5	0.8	25.6	-0.8	-	-	-1.1	-	11.8	17.6
	W	-	1.2	-	1.2	-2.8	0.9	0.1	1.1	0.1	-	-	0.0	-	0.8	1.5
	T	**-3.7**	**18.7**	**20.7**	**-9.0**	**2.0**	**18.4**	**0.9**	**26.7**	**-0.7**	**2.8**	**15.8**	**-1.1**	**-1.8**	**12.6**	**19.1**
WHITEHORSE	H	-	14.6	-	-12.2	3.3	14.8	0.1	21.1	-1.8	-	-	0.1	-	9.8	14.7
	W	-	0.7	-	0.7	-1.9	0.6	0.1	0.6	0.0	-	-	-0.1	-	0.6	0.9
	T	**-6.4**	**15.3**	**17.0**	**-11.5**	**1.4**	**15.4**	**0.2**	**21.7**	**-1.8**	**1.5**	**12.2**	**0.0**	**-2.3**	**10.4**	**15.6**
KOTZEBUE	H	-	19.7	-	-12.8	6.6	20.0	0.9	23.5	-1.3	-	-	-0.6	-	13.8	19.9
	W	-	0.7	-	0.7	-1.7	0.6	0.1	0.7	0.0	-	-	0.0	-	0.6	1.1
	T	**-4.2**	**20.4**	**19.3**	**-12.1**	**4.9**	**20.6**	**1.0**	**24.2**	**-1.3**	**4.7**	**11.9**	**-0.7**	**-5.1**	**14.4**	**21.0**
ALERT	H	-	22.2	-	-15.4	9.1	22.5	1.8	20.6	-1.4	-	-	-2.2	-	16.1	22.4
	W	-	0.5	-	0.5	-0.8	0.1	0.1	0.5	0.1	-	-	0.0	-	0.1	1.6
	T	**-3.5**	**22.7**	**17.1**	**-14.9**	**8.3**	**22.6**	**1.9**	**21.2**	**-1.3**	**7.3**	**8.8**	**-2.2**	**-8.1**	**16.2**	**24.0**

Table 6 - Mapping function mean error at 15 degrees elevation angle; otherwise, as for Table 5.

STATION		MAPPING FUNCTION														
		BB	BL	BE	CH	DA	GG	HE	HM	IF	LA	MM	NI	SA	ST	YI
SAN JUAN	H	-	41.6	-	10.9	7.1	41.0	0.5	96.3	-3.3	-	-	0.2	-	23.6	44.6
	W	-	11.6	-	11.7	-27.7	12.4	0.0	10.7	0.8	-	-	0.7	-	11.4	13.9
	T	**27.2**	**53.2**	**62.4**	**22.6**	**-20.6**	**53.4**	**0.5**	**107.0**	**-2.5**	**-7.5**	**81.6**	**0.9**	**-9.1**	**35.0**	**58.5**
GUAM	H	-	39.6	-	11.6	6.2	38.9	0.7	95.7	-3.0	-	-	1.3	-	22.1	42.5
	W	-	12.4	-	12.5	-28.6	13.2	0.6	11.5	1.4	-	-	1.0	-	12.2	14.9
	T	**30.7**	**52.0**	**61.7**	**24.1**	**-22.4**	**52.1**	**1.3**	**107.2**	**-1.6**	**-8.1**	**83.0**	**2.3**	**-8.3**	**34.3**	**57.4**
NASHVILLE	H	-	45.6	-	2.1	11.3	45.7	1.6	85.8	-1.6	-	-	-1.4	-	28.3	48.9
	W	-	6.6	-	6.7	-15.3	6.1	0.4	6.1	0.6	-	-	0.5	-	5.8	8.0
	T	**1.6**	**52.2**	**60.4**	**8.8**	**-4.0**	**51.8**	**2.0**	**91.9**	**-1.0**	**-0.4**	**63.4**	**-0.9**	**-1.9**	**34.1**	**56.9**
DENVER	H	-	31.7	-	-10.1	6.0	31.8	1.3	60.2	-2.7	-	-	-0.1	-	19.3	34.6
	W	-	2.4	-	2.5	-7.8	2.2	0.5	2.2	0.2	-	-	-0.5	-	2.2	3.1
	T	**-12.6**	**34.1**	**42.2**	**-7.6**	**-1.8**	**34.0**	**1.8**	**62.4**	**-2.5**	**-3.2**	**46.2**	**-0.6**	**6.6**	**21.5**	**37.7**
OAKLAND	H	-	47.2	-	4.1	11.7	47.4	1.7	89.4	-1.1	-	-	0.4	-	29.4	50.5
	W	-	4.7	-	4.8	-11.8	5.9	-0.1	4.4	0.1	-	-	0.1	-	5.7	5.8
	T	**9.2**	**51.9**	**66.1**	**8.9**	**-0.1**	**53.3**	**1.6**	**93.8**	**-1.0**	**-0.1**	**60.1**	**0.5**	**-3.0**	**35.1**	**56.3**
ST. JOHN'S	H	-	53.5	-	-5.4	18.6	54.1	3.2	78.2	-1.0	-	-	-2.7	-	35.9	57.2
	W	-	4.0	-	4.1	-8.8	3.0	0.5	3.7	0.3	-	-	0.1	-	2.8	4.9
	T	**-4.1**	**57.5**	**57.2**	**-1.3**	**9.8**	**57.1**	**3.7**	**81.9**	**-0.7**	**8.2**	**47.9**	**-2.6**	**-8.7**	**38.7**	**62.1**
WHITEHORSE	H	-	44.4	-	-13.7	13.5	45.4	1.0	64.0	-4.1	-	-	0.8	-	29.4	47.9
	W	-	2.3	-	2.3	-5.9	1.9	0.3	2.1	0.1	-	-	-0.4	-	1.8	2.9
	T	**-12.5**	**46.7**	**46.0**	**-11.4**	**7.6**	**47.3**	**1.3**	**66.1**	**-4.0**	**4.0**	**36.4**	**0.4**	**-9.6**	**31.2**	**50.8**
KOTZEBUE	H	-	60.4	-	-13.4	24.1	61.7	3.9	71.4	-2.5	-	-	-1.5	-	42.1	64.4
	W	-	2.4	-	2.5	-5.2	1.9	0.2	2.3	0.1	-	-	-0.1	-	1.9	3.0
	T	**-5.8**	**62.8**	**52.7**	**-10.9**	**18.9**	**63.6**	**4.1**	**73.7**	**-2.4**	**14.0**	**35.3**	**-1.6**	**-19.6**	**44.0**	**67.4**
ALERT	H	-	68.1	-	-21.7	31.8	69.7	6.7	62.5	-2.7	-	-	-6.3	-	49.3	72.4
	W	-	1.6	-	1.6	-2.5	0.4	0.4	1.5	0.2	-	-	0.1	-	0.4	1.9
	T	**-4.5**	**69.7**	**45.9**	**-20.1**	**29.3**	**70.1**	**7.1**	**64.0**	**-2.5**	**22.2**	**25.3**	**-6.2**	**-29.2**	**49.7**	**74.3**

Table 7 - Mapping function mean error at 10 degrees elevation angle; otherwise, as for Table 5.

STATION		MAPPING FUNCTION														
		BB	BL	BE	CH	DA	GG	HE	HM	IF	LA	MM	NI	SA	ST	YI
SAN JUAN	H	-	554	-	792	623	562	5	279	-15	-	-	4	-	285	571
	W	-	288	-	281	-405	269	7	192	26	-	-	16	-	244	300
	T	**13014**	**842**	**-537**	**1073**	**218**	**831**	**12**	**471**	**11**	**293**	**178**	**20**	**-6834**	**529**	**871**
GUAM	H	-	525	-	792	609	531	6	286	-13	-	-	19	-	265	541
	W	-	308	-	301	-413	289	21	209	41	-	-	22	-	262	321
	T	**12485**	**833**	**-534**	**1093**	**196**	**820**	**27**	**495**	**28**	**274**	**222**	**41**	**-6712**	**527**	**862**
NASHVILLE	H	-	616	-	649	622	632	30	147	13	-	-	-13	-	349	635
	W	-	163	-	160	-226	131	12	109	18	-	-	13	-	122	171
	T	**18835**	**779**	**-456**	**809**	**396**	**763**	**42**	**256**	**31**	**413**	**-86**	**0**	**-6911**	**471**	**806**
DENVER	H	-	422	-	372	457	435	29	-51	-8	-	-	9	-	230	439
	W	-	63	-	62	-120	49	11	37	5	-	-	-10	-	47	67
	T	**21534**	**485**	**-473**	**434**	**337**	**484**	**40**	**-14**	**-3**	**279**	**-140**	**-1**	**-5791**	**277**	**506**
OAKLAND	H	-	641	-	696	643	659	37	184	25	-	-	18	-	368	661
	W	-	117	-	115	-179	130	-1	76	5	-	-	1	-	124	123
	T	**18221**	**758**	**-368**	**811**	**464**	**789**	**36**	**260**	**30**	**449**	**-178**	**19**	**-7117**	**492**	**784**
ST. JOHN'S	H	-	726	-	528	669	748	55	26	21	-	-	-36	-	447	748
	W	-	98	-	97	-132	68	10	66	8	-	-	3	-	65	104
	T	**19630**	**824**	**-470**	**625**	**537**	**816**	**65**	**92**	**29**	**536**	**-353**	**-33**	**-7197**	**512**	**852**
WHITE HORSE	H	-	592	-	355	551	617	23	-113	-35	-	-	13	-	351	612
	W	-	56	-	55	-92	40	5	35	1	-	-	-9	-	39	60
	T	**20623**	**648**	**-534**	**410**	**459**	**657**	**28**	**-78**	**-34**	**422**	**-446**	**4**	**-6828**	**390**	**672**
KOTZEBUE	H	-	830	-	410	709	859	75	-100	0	-	-	-22	-	528	853
	W	-	58	-	58	-80	40	3	39	2	-	-	-3	-	39	62
	T	**18983**	**888**	**-536**	**468**	**629**	**899**	**78**	**-61**	**2**	**629**	**-580**	**-25**	**-7535**	**567**	**915**
ALERT	H	-	956	-	278	777	986	131	-227	5	-	-	-94	-	635	979
	W	-	36	-	36	-39	10	7	26	3	-	-	1	-	10	39
	T	**17470**	**992**	**-612**	**314**	**738**	**996**	**138**	**-201**	**8**	**744**	**-723**	**-93**	**-7628**	**645**	**1018**

Table 8 - Mapping function mean error at 3 degrees elevation angle; otherwise, as for Table 5.

		MAPPING FUNCTION														
STATION	ε	BB	BL	BE	CH	DA	GG	HE	HM	IF	LA	MM	NI	SA	ST	YI
SAN JUAN	30	0.3	0.1	0.1	0.1	0.2	0.1	0.1	0.1	0.1	0.1	0.2	0.1	0.1	0.1	1.8
	15	2.7	1.1	0.7	1.1	1.7	0.8	0.6	1.0	0.6	0.9	1.7	0.5	1.0	0.8	1.1
	10	7.9	3.4	2.5	3.6	5.3	2.5	2.0	3.4	1.9	2.8	5.6	1.7	3.3	2.4	3.7
	3	1111	72	59	77	63	41	36	64	35	44	104	34	72	38	73
GUAM	30	0.3	0.2	0.1	0.2	0.3	0.1	0.1	0.1	0.1	0.1	0.2	0.1	0.1	0.1	1.2
	15	2.7	1.4	0.9	1.4	1.8	0.9	0.8	1.3	0.7	0.8	2.1	0.7	1.1	0.8	1.6
	10	8.1	4.7	3.2	4.7	5.5	2.7	2.4	4.3	2.3	2.5	6.9	2.4	3.4	2.6	5.2
	3	958	106	78	105	67	47	49	86	49	38	132	48	89	43	109
NASHVILLE	30	0.6	0.3	0.1	0.3	0.6	0.3	0.2	0.3	0.1	0.3	0.5	0.1	0.2	0.2	1.4
	15	5.0	2.3	1.1	2.9	4.5	2.1	1.3	2.9	1.0	2.7	4.2	1.1	1.6	2.0	2.3
	10	14.5	7.0	3.5	9.5	14.0	6.7	4.1	9.2	3.3	8.5	13.3	3.7	5.4	6.3	7.2
	3	3591	110	85	173	164	97	67	148	56	135	220	63	194	88	112
DENVER	30	0.6	0.3	0.2	0.2	0.5	0.3	0.1	0.3	0.1	0.3	0.4	0.1	0.3	0.3	0.7
	15	4.6	2.4	1.3	2.2	3.4	2.6	1.3	2.2	0.9	2.7	3.0	0.9	2.4	2.5	2.4
	10	13.2	7.5	4.0	7.1	10.4	8.3	4.0	7.0	2.8	8.2	9.7	2.8	7.7	7.8	7.7
	3	4358	106	64	125	115	122	61	113	48	111	162	50	162	112	107
OAKLAND	30	0.5	0.2	0.2	0.3	0.3	0.2	0.2	0.3	0.2	0.2	0.3	0.1	0.2	0.2	0.7
	15	4.3	2.1	1.9	2.2	2.4	2.1	1.7	2.2	1.6	2.0	2.6	1.1	2.1	2.0	2.1
	10	12.6	6.6	6.1	7.1	7.5	6.6	5.4	7.1	5.1	6.4	8.4	3.5	6.7	6.4	6.7
	3	2409	105	98	117	100	103	84	111	81	97	134	60	129	99	106
ST. JOHN'S	30	0.4	0.2	0.2	0.4	0.4	0.4	0.1	0.4	0.1	0.2	0.5	0.2	0.3	0.4	1.0
	15	3.6	1.7	1.8	3.1	2.9	3.0	1.2	3.2	1.1	1.8	4.5	1.4	2.7	2.9	2.1
	10	10.5	5.2	5.6	10.1	9.1	8.4	3.8	10.1	3.6	5.8	14.4	4.5	8.5	8.2	5.4
	3	1991	90	73	177	104	88	64	159	61	92	236	76	229	83	92
WHITEHORSE	30	0.3	0.4	0.2	0.3	0.5	0.3	0.2	0.3	0.1	0.4	0.4	0.2	0.3	0.3	0.5
	15	2.7	3.1	1.5	2.3	3.8	2.9	1.5	2.4	1.1	3.4	3.2	1.6	2.7	2.7	3.3
	10	7.8	9.6	4.7	7.5	11.9	9.2	4.7	7.6	3.5	10.2	10.4	4.9	8.7	8.5	10.0
	3	2562	145	57	128	135	135	74	118	59	144	168	73	167	118	146
KOTZEBUE	30	0.3	0.4	0.2	0.4	0.6	0.4	0.2	0.4	0.2	0.4	0.5	0.2	0.4	0.3	0.6
	15	2.6	3.4	2.1	3.3	4.6	3.2	1.5	3.3	1.3	3.7	4.2	1.7	3.1	2.9	3.8
	10	7.6	10.7	6.3	10.4	14.4	10.1	4.9	10.3	4.0	11.5	13.4	5.3	9.9	9.0	10.9
	3	1709	159	74	174	164	146	77	161	65	172	212	79	209	121	159
ALERT	30	0.2	0.4	0.4	0.4	0.5	0.3	0.2	0.4	0.2	0.4	0.5	0.4	0.5	0.3	0.3
	15	1.9	3.1	3.0	3.7	3.7	2.7	1.3	3.7	1.3	3.1	4.3	3.4	4.5	2.4	4.0
	10	5.4	9.7	9.3	11.5	11.6	8.7	4.1	11.5	4.0	9.9	13.4	10.6	14.3	7.5	9.9
	3	2418	163	114	171	138	142	65	164	56	155	197	148	188	114	161

Table 9 - Root-mean-square (rms) scatters about the mean of the differences between the delays computed using the mapping functions and the ray trace results for various elevation angles, in millimetres.
Note: Only the rms for the total tropospheric delay is shown.

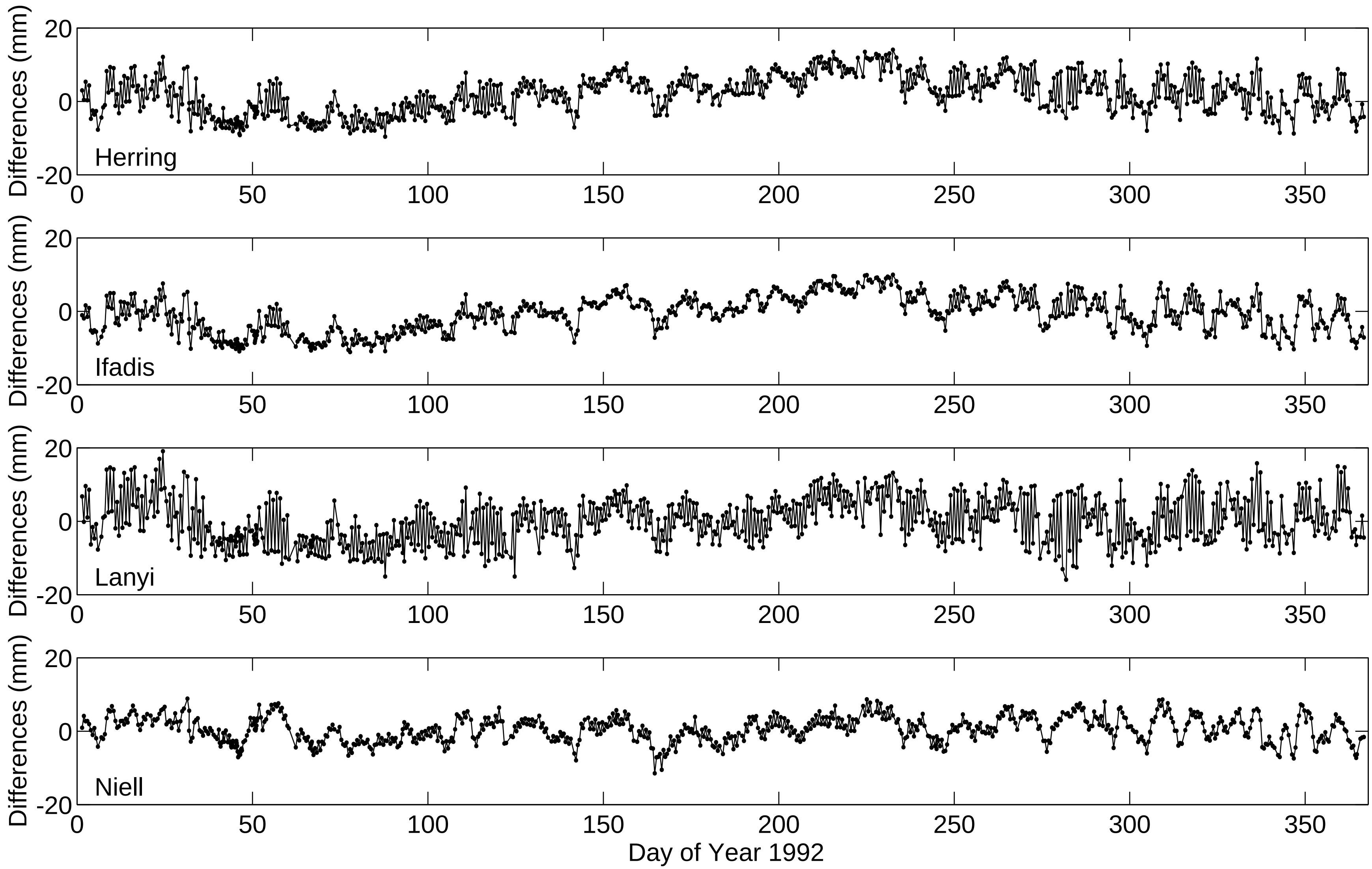

Figure 1 - Differences between the delay computed using the HE, IF, LA, and NI mapping functions and the ray-trace results, for the total delay at 10° elevation angle, for Oakland. This station is affected by frequent temperature inversions, a phenomenon which degrades the performance of the mapping functions using the surface temperature as an input parameter, such as the Lanyi, Herring, and Ifadis mapping functions. The latter is the least affected of these three. The independence of the Niell functions from the meteorological parameters is reflected in a smaller rms scatter, for this station.